A switching control approach for the robust practical stabilization of a unicycle-like marine vehicle under non-vanishing perturbations

Dimitra Panagou and Kostas J. Kyriakopoulos

***Abstract*— This paper presents a solution to the robust practical stabilization of a unicycle-like marine vehicle, under non-vanishing current-induced perturbations. A hysteresis-based switching control strategy is proposed, rendering the system globally practically stable to a set G around the origin. The control scheme consists of three control laws; the first one is active out of G and drives the system trajectories into G, based on a dipole-like vector field. The other two control laws are active in G and alternately regulate the position and the orientation of the vehicle. The system is shown to be robust, in the sense that the vehicle enters and remains into G even if the current is unknown and only its maximum bound is given. The efficacy of the proposed solution is demonstrated through simulation results.**

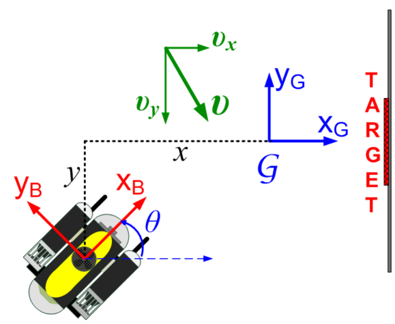

Fig. 1. The marine vehicle should be driven and remain into a neighborhood of the origin $\boldsymbol{q_G} = [0\ 0\ 0]^{\mathrm{T}}$ despite the effect of the current disturbance $\boldsymbol{v}$

I. INTRODUCTION

Nonholonomic stabilization problems arise in a wide range of robotic applications, since a large class of such systems, including mobile robots and underactuated robotic vehicles (marine, aerial) are subject to nonholonomic constraints. The literature is abundant in control solutions for nonholonomic systems with catastatic Pfaffian constraints[1]. In this case, control laws are usually designed under the assumptions that no model uncertainty, or no additive disturbances apply.

However, these assumptions are often unrealistic for real world applications. Therefore, the development of stabilizing solutions with robustness considerations has been of increasing interest. In particular, the regulation of nonholonomic systems with external disturbances, which may be either vanishing [1]–[8] or non-vanishing [9]–[15] at the origin, has received special attention. In the latter case, it is usually assumed that the disturbances are small and bounded, or that the perturbation vector field satisfies certain conditions.

A typical example where external disturbances serve as non-vanishing perturbations at a desired configuration is the dynamic positioning of underactuated marine vehicles in the presence of environmental disturbances [16]–[19]. The external disturbances are usually modeled as a constant (current or wind) velocity disturbance, and the main idea is to control the vehicle so that its final orientation is aligned with the direction of the current.

Nevertheless, allowing the orientation to be ruled by external disturbances is often not acceptable, either for safety, or for performance reasons. One such example, that we consider in this paper, is the case of a unicycle-like marine vehicle, which inspects a stationary target with an onboard camera under the presence of a current disturbance $\boldsymbol{v}$ (Fig. 1). For the inspection task to be effective, the vehicle is required to converge to the origin $\boldsymbol{q_G} = \begin{bmatrix}0 & 0 & 0\end{bmatrix}^{\mathrm{T}}$ of the global frame $\mathcal{G}$. However, the perturbation induced by the current is non-vanishing at $\boldsymbol{q_G}$, and thus the origin is not an equilibrium point. Consequently, it is meaningless to search for control laws that yield the system asymptotically stable at $\boldsymbol{q_G}$. Instead, one can aim at rendering the system ultimately bounded within a set that contains the origin, addressing thus the practical stabilization problem.

This paper proposes a hysteresis-based switching control strategy that yields global practical stability for a unicycle-like marine vehicle, under current-induced non-vanishing perturbations. Under the proposed control scheme, the vehicle converges and remains into a set G around the origin. The resulting performance is achieved via state-based switching among three controllers. The first controller is active outside the set G, and drives the system trajectories into G using a dipole-like vector field [20]. The other two controllers are active inside G, and alternately regulate the position and the orientation of the vehicle. The system is shown to be robust, in the sense that the system trajectories enter and remain into G even when only a maximum bound $\|\boldsymbol{v}\|_{\max}$ on the current disturbance is given. In contrast to earlier relevant work on dynamic positioning [16]–[19] which drop the specification on the desired orientation, the proposed control strategy allows also for the regulation of the vehicle's orientation to zero, during the time intervals when the corresponding controller is active. This feature, along with the robustness property, renders the proposed solution suitable for applications where both the position and orientation of a robot are critical, e.g. for inspection tasks.

The paper is organized as follows: Section II gives the

The authors are with the Control Systems Lab, School of Mechanical Engineering, National Technical University of Athens, Greece {dpanagou, kkyria}@mail.ntua.gr

[1]Pfaffian constraints are of the form $\boldsymbol{A}(\boldsymbol{q})\dot{\boldsymbol{q}} = \boldsymbol{b}(\boldsymbol{q})$, where $\boldsymbol{q} \in \mathbb{R}^n$ is the system state vector, $\boldsymbol{A}(\boldsymbol{q}) \in \mathbb{R}^{\kappa \times n}$ and $\boldsymbol{b}(\boldsymbol{q}) \in \mathbb{R}^{\kappa}$. If $\boldsymbol{b}(\boldsymbol{q}) = \boldsymbol{0}$ the constraints are catastatic, whereas if $\boldsymbol{b}(\boldsymbol{q}) \neq \boldsymbol{0}$ the constraints are acatastatic

problem formulation and Section III presents the switching strategy. The construction of the control laws, the stability analysis and the robustness consideration are given in Section IV. Section V includes the simulation results. The conclusions and thoughts on future research are summarized in Section VI.

II. Problem Formulation

Consider a marine vehicle (underwater or surface) which has two back thrusters for the motion on the horizontal plane, but no thruster along the lateral degree-of-freedom (d.o.f.). In order to simplify the control design, the vehicle is modeled as a unicycle[2]. The vehicle moves under the influence of an non-rotational current $\boldsymbol{v}$, with components v_x, v_y with respect to (w.r.t.) the global frame $\mathcal{G}$. The equations of motion are

$$\dot{\boldsymbol{q}} = \boldsymbol{v} + \boldsymbol{G}(\boldsymbol{q})\boldsymbol{u} \Rightarrow \begin{bmatrix} \dot{x} \\ \dot{y} \\ \dot{\theta} \end{bmatrix} = \begin{bmatrix} v_x \\ v_y \\ 0 \end{bmatrix} + \begin{bmatrix} \cos\theta & 0 \\ \sin\theta & 0 \\ 0 & 1 \end{bmatrix} \begin{bmatrix} u_1 \\ u_2 \end{bmatrix}, \quad (1)$$

where $\boldsymbol{q} = \begin{bmatrix} x & y & \theta \end{bmatrix}^{\mathrm{T}}$ is the state vector, x, y are the position coordinates and θ is the orientation of the vehicle w.r.t. $\mathcal{G}$, $\boldsymbol{u} = \begin{bmatrix} u_1 & u_2 \end{bmatrix}^{\mathrm{T}}$ is the vector of control inputs, u_1, u_2 are the linear and the angular velocity of the vehicle w.r.t. the body-fixed frame $\mathcal{B}$, and $\boldsymbol{v} = \begin{bmatrix} v_x & v_y & 0 \end{bmatrix}^{\mathrm{T}}$ is the perturbation vector field. Since $\boldsymbol{v}(t, \boldsymbol{q_G}) \neq 0 \ \forall t \geq 0$, $\boldsymbol{v}$ is a non-vanishing perturbation at the origin. The $\kappa = 1$ acatastatic Pfaffian constraint of (1) is:

$$\underbrace{\begin{bmatrix} -\sin\theta & \cos\theta & 0 \end{bmatrix}}_{\boldsymbol{a}^{\mathrm{T}}(\boldsymbol{q})} \begin{bmatrix} \dot{x} \\ \dot{y} \\ \dot{\theta} \end{bmatrix} = -v_x \sin\theta + v_y \cos\theta \Rightarrow \boldsymbol{a}^{\mathrm{T}}(\boldsymbol{q})\dot{\boldsymbol{q}} = b(\boldsymbol{q}),$$

where $b(\boldsymbol{q}) \neq 0$ can be seen as a violation of the catastatic constraint of the unicycle. Using the Frobenius theorem one can verify that the constraint is non-integrable. The constraint equation implies that $\dot{\boldsymbol{q}}_{\boldsymbol{e}} = \boldsymbol{0}$, i.e. that $\boldsymbol{q_e}$ is an equilibrium of (1), if and only if $b(\boldsymbol{q_e}) = 0 \Rightarrow -v_x \sin\theta_e + v_y \cos\theta_e = 0$. As expected, the orientation θ_e at the equilibrium depends on $\boldsymbol{v}$. The origin $\boldsymbol{q_G} = \boldsymbol{0}$ is an equilibrium point of (1) if and only if $v_y = 0$, whereas if $v_y \neq 0$, the system can only be ultimately bounded in a neighborhood of the origin.

Problem Statement: Given the perturbed nonholonomic system (1), design a switching signal $\sigma(\cdot) : \mathbb{R}^n \rightarrow \mathcal{I} = \{1, 2, \ldots, \chi\}$ and χ feedback control laws $\boldsymbol{u} = \boldsymbol{\psi}_\sigma(t, \boldsymbol{q})$, so that (1) is ε-practically asymptotically stable around the origin, in the sense that for given $\varepsilon > 0$ and any initial $\boldsymbol{q}_0$, the solution $\boldsymbol{q}(t) = \boldsymbol{q}(t, \boldsymbol{q}_0, \boldsymbol{u})$ exists $\forall t \geq 0$, and $\boldsymbol{q}(t) \in \mathcal{B}(\boldsymbol{0}, \varepsilon)$, $\forall t \geq T$, where $T = T(\boldsymbol{q}_0) > 0$.

III. Switching Control Strategy

The proposed control scheme employs the concept of dipole-like vector fields. For the unicycle, the idea is that the system is controlled to follow the flow lines of the vector field $\mathbf{F}_{\boldsymbol{n}}$ (Fig. 2(a)), which converge to $(x, y) = (0, 0)$ with orientation $\theta_{\boldsymbol{n}} \rightarrow 0$. In the same context, one can construct a dipole-like vector field $\mathbf{F}_{\boldsymbol{p}} = \mathrm{F}_{px}\,\hat{\boldsymbol{x}} + \mathrm{F}_{py}\,\hat{\boldsymbol{y}}$ for the perturbed system (1), whose flow lines converge to the equilibrium $\boldsymbol{q_e}$. The analytic form of the vector field $\mathbf{F}_{\boldsymbol{p}}$ (Fig. 2(b)) is given by the dipole-like field in [20] as

$$\mathrm{F}_{px} = \lambda(v_x x + v_y y)x - v_x + v_x e^{-(x^2+y^2)}, \quad (2a)$$

$$\mathrm{F}_{py} = \lambda(v_x x + v_y y)y - v_y + v_y e^{-(x^2+y^2)}. \quad (2b)$$

Given the vector field $\mathbf{F}_{\boldsymbol{p}}$, one can design a control law

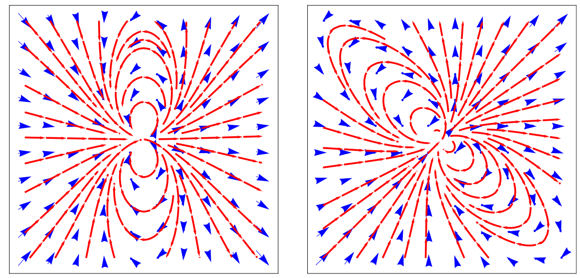

(a) The nominal field $\mathbf{F}_{\boldsymbol{n}}$ (b) The perturbed field $\mathbf{F}_{\boldsymbol{p}}$

Fig. 2. The fields $\mathbf{F}_{\boldsymbol{n}}(x, y)$ and $\mathbf{F}_{\boldsymbol{p}}(x, y)$ for $\lambda = 3$, $\boldsymbol{p_n} = \begin{bmatrix} p_1 & 0 \end{bmatrix}^{\mathrm{T}}$, $\boldsymbol{p_p} = \begin{bmatrix} p_1 & v_y \end{bmatrix}^{\mathrm{T}}$, $p_1 = v_x = 1$ m/sec, $v_y = 1$ m/sec.

$\boldsymbol{u} = \boldsymbol{\psi}_1(\boldsymbol{q})$ that forces (1) to follow the flow lines. Then, the position $\boldsymbol{r} = \begin{bmatrix} x & y \end{bmatrix}^{\mathrm{T}}$ converges to the origin, however the orientation θ converges to the orientation φ of the field. Denote $\boldsymbol{q} = \begin{bmatrix} \boldsymbol{r}^{\mathrm{T}} & \theta \end{bmatrix}^{\mathrm{T}}$. Inspired by [21], we say that the subsystem $\boldsymbol{f}_1(\boldsymbol{q}, \boldsymbol{\psi}_1)$ is stable w.r.t. $\boldsymbol{r}$ and unstable w.r.t. θ. Controlling the orientation θ as well, so that $\theta \rightarrow 0$, requires a compromise on a subsystem $\boldsymbol{f}_2(\boldsymbol{q}, \boldsymbol{\psi}_2)$ of stable θ, but unstable $\boldsymbol{r}$. Switching properly between these subsystems may yield an ε-practically stable system.

We partition the configuration space $\mathcal{C} \subseteq \mathbb{R}^2 \times [0, 2\pi)$ into the regions K and G, $K = \{\begin{bmatrix} \boldsymbol{r}^{\mathrm{T}} & \theta \end{bmatrix}^{\mathrm{T}} \in \mathcal{C} \mid \|\boldsymbol{r}\| > r_0\}$ and $G = \mathcal{C} \setminus K$, where $r_0 > 0$ should satisfy the conditions (7) and (8), see Section IV. The region K is divided into $A = \{\boldsymbol{q} \in K \mid \langle \boldsymbol{r}, \boldsymbol{v} \rangle \geq 0\}$ and $B = \{\boldsymbol{q} \in K \mid \langle \boldsymbol{r}, \boldsymbol{v} \rangle < 0\}$, with $K = (A \cup B)$ (Fig. 3). The region G is divided into G_1 and G_2, where $G_1 = \{\boldsymbol{q} \in G \mid \langle \boldsymbol{r}, \boldsymbol{v} \rangle \geq 0\}$, $G_2 = \{\boldsymbol{q} \in G \mid \langle \boldsymbol{r}, \boldsymbol{v} \rangle < 0\}$ and $G = (G_1 \cup G_2)$. When $\boldsymbol{q} \in G_1$, the disturbance $\boldsymbol{v}$ forces the position $\boldsymbol{r}$ of the (uncontrolled) system (1) away from the origin, whereas when $\boldsymbol{q} \in G_2$, the disturbance forces the position $\boldsymbol{r}$ towards the origin.

The idea for the control design is that if $\boldsymbol{q} \in K$, a control law based on the vector field (2) drives the system into the set G. Then, while $\boldsymbol{q} \in G$, the system switches to a control law that regulates the orientation $\theta \rightarrow 0$. Since the regulation

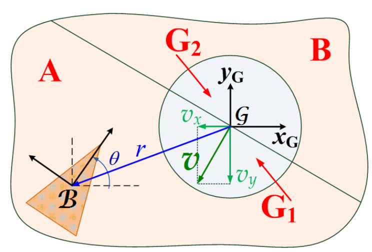

Fig. 3. Operating regions and system description w.r.t. frame $\mathcal{G}$

[2]The resulting kinematic controllers can then be backstepped into the dynamics of an underactuated marine vehicle

of θ may yield instability w.r.t. the position $\boldsymbol{r}$, it is preferable to control θ when $\boldsymbol{v}$ forces $\boldsymbol{r}$ towards the origin, i.e. when $\boldsymbol{q} \in G_2$. Thus, if the system trajectory $\boldsymbol{q}(t)$ enters G_1 after leaving K, an additional control law is needed to drive $\boldsymbol{q}(t)$ into G_2. This consideration results into switching among $\chi = 3$ controllers $\boldsymbol{\psi}_\sigma(\boldsymbol{q})$, $\sigma \in \{1,2,3\}$: $\boldsymbol{\psi}_1(\boldsymbol{q})$ forces the system into G, $\boldsymbol{\psi}_2(\boldsymbol{q})$ forces the system into G_2 in the case that $\boldsymbol{r}$ has reached G_1 and $\boldsymbol{\psi}_3(\boldsymbol{q})$ regulates $\theta \to 0$ in the case that $\boldsymbol{r}$ has reached G_2. More specifically, we propose the following hysteresis-based switching logic.

- If $\boldsymbol{q}(0) \in K$, then $\sigma(\boldsymbol{q}(0)) = 1$, else $\sigma(\boldsymbol{q}(0)) = 3$.
- If $\boldsymbol{q}(t) \in K$ and $\sigma(\boldsymbol{q}(t^-)) = 1$, then $\sigma(\boldsymbol{q}(t)) = 1$.
- If $\boldsymbol{q}(t) \in G_1$ and $\sigma(\boldsymbol{q}(t^-)) = 1$, then $\sigma(\boldsymbol{q}(t)) = 2$.
- If $\boldsymbol{q}(t) \in G_2$ and $\sigma(\boldsymbol{q}(t^-)) = 1$, then $\sigma(\boldsymbol{q}(t)) = 3$.
- If $\boldsymbol{q}(t) \in G$ and $\sigma(\boldsymbol{q}(t^-)) = 2$, then $\sigma(\boldsymbol{q}(t)) = 2$.
- If $\boldsymbol{q}(t) \in B$ and $\sigma(\boldsymbol{q}(t^-)) = 2$, then $\sigma(\boldsymbol{q}(t)) = 3$.
- If $\boldsymbol{q}(t) \in B$ and $\sigma(\boldsymbol{q}(t^-)) = 3$, then $\sigma(\boldsymbol{q}(t)) = 3$.
- If $\boldsymbol{q}(t) \in G$ and $\sigma(\boldsymbol{q}(t^-)) = 3$, then $\sigma(\boldsymbol{q}(t)) = 3$.
- If $\boldsymbol{q}(t) \in A$ and $\sigma(\boldsymbol{q}(t^-)) = 3$, then $\sigma(\boldsymbol{q}(t)) = 1$.

The hysteresis-based logic prevents the appearance of chattering when the state crosses the switching surfaces.

IV. Control Design

A. Design of the control law $\boldsymbol{u} = \boldsymbol{\psi}_1(\boldsymbol{q})$

Lemma 1: The position $\boldsymbol{r} = \begin{bmatrix} x & y \end{bmatrix}^{\mathrm{T}}$ of the perturbed system (1) enters a ball $\mathcal{B}(\mathbf{0}, r_0)$ of the origin for any $\boldsymbol{r}(0) \notin \mathcal{B}(\mathbf{0}, r_0)$, under the control input $\boldsymbol{\psi}_1 = \begin{bmatrix} u_1 & u_2 \end{bmatrix}^{\mathrm{T}}$,

$$u_1 = -k_1 \operatorname{sgn}\!\left(\boldsymbol{r}^{\mathrm{T}} \left[\begin{smallmatrix} \cos\theta \\ \sin\theta \end{smallmatrix}\right]\right) \|\boldsymbol{r}\| - \operatorname{sgn}(\boldsymbol{r}^{\mathrm{T}} \boldsymbol{v}) \operatorname{sgn}(\boldsymbol{p}^{\mathrm{T}} \boldsymbol{r}) \|\boldsymbol{v}\| , \tag{3a}$$

$$u_2 = -k_2(\theta - \varphi) + \dot{\varphi}, \tag{3b}$$

where $k_1, k_2 > 0$, $\varphi = \operatorname{atan2}(\mathrm{F}_{py}, \mathrm{F}_{px})$ is the orientation of the vector field (2) at (x, y), $\operatorname{sgn}(\cdot)$ is defined as $\operatorname{sgn}(a) = 1$ if $a \geq 0$, and $\operatorname{sgn}(a) = -1$ if $a < 0$, and r_0 is chosen to satisfy (7) and (8). The proof is given in the Appendix A.

B. Design of the control laws $\boldsymbol{u} = \boldsymbol{\psi}_2(\boldsymbol{q}), \boldsymbol{u} = \boldsymbol{\psi}_3(\boldsymbol{q})$

Denote ∂X_Y the boundary of a set X w.r.t. a neighbor set Y. Once $\boldsymbol{q}(t)$ has entered $G = \{\boldsymbol{q} = \begin{bmatrix} \boldsymbol{r}^{\mathrm{T}} & \theta \end{bmatrix}^{\mathrm{T}} \in \mathcal{B}(\mathbf{0}, r_0) \times [0, 2\pi)\}$, consider the following two cases.

1) $\boldsymbol{q} \in G_1 = \{G \mid \langle \boldsymbol{r}, \boldsymbol{v} \rangle \geq 0\}$: Assume that $\boldsymbol{q}(t)$ has entered G_1, where $\boldsymbol{v}$ drives the system away from the origin.

Lemma 2: The system trajectory $\boldsymbol{q}(t)$ enters G_2, where $\langle \boldsymbol{r}, \boldsymbol{v} \rangle < 0$, under the control law $\boldsymbol{\psi}_2 = \begin{bmatrix} u_1 & u_2 \end{bmatrix}^{\mathrm{T}}$,

$$u_1 = -k_3 \operatorname{sgn}(v_x) \|\boldsymbol{v}\|, \quad u_2 = -k_4(\theta - \theta_{\boldsymbol{p}}), \tag{4}$$

with $k_3 > 1$, $k_4 > 0$. The proof is given in the Appendix B.

2) $\boldsymbol{q} \in G_2 = \{G \mid \langle \boldsymbol{r}, \boldsymbol{v} \rangle < 0\}$: Assume that $\boldsymbol{q}(t)$ has entered G_2, where $\boldsymbol{v}$ drives the system towards the origin. The system is controlled so that $\theta \to 0$ under the control law

$$\boldsymbol{\psi}_3 = \begin{bmatrix} 0 & u_{23} \end{bmatrix}^{\mathrm{T}}, \text{ where } u_{23} = -k_5\theta, \ k_5 > 0. \tag{5}$$

It is easy to verify that $\boldsymbol{r}(t)$ enters G_1 by considering the function $V_{31} = -\boldsymbol{r}^{\mathrm{T}} \boldsymbol{v}$, which is positive for $\boldsymbol{r} \in G_2$ and zero on $\partial G_{2_{G_1}}$, whose time derivative is $\dot{V}_{31} = -v_x(u_1 \cos\theta + v_x) - v_y(u_1 \sin\theta + v_y) = -{v_x}^2 - {v_y}^2$. Furthermore, taking $V_{32} = {r_0}^2 - x^2 - y^2$, where $\dot{V}_{32} = -2\boldsymbol{r}^{\mathrm{T}} \boldsymbol{v} < 0$ for $\boldsymbol{r} \in G_1$, verifies that $\boldsymbol{q}(t)$ also enters A.

C. Stability of the switched system $\dot{\boldsymbol{q}} = \boldsymbol{f}_\sigma(\boldsymbol{q}, \boldsymbol{\psi}_\sigma)$

Following [22], consider a strictly increasing sequence of times $\mathrm{T} = \{t_0, t_1, \ldots, t_n, \ldots,\}$ and the switching sequence

$$\Sigma = \{\boldsymbol{q}_0; (\iota_0, t_0), (\iota_1, t_1), \ldots, (\iota_n, t_n), \ldots \mid \iota_n \in \mathcal{I}, n \in \mathbb{N}\},$$

where t_0 is the initial time, $\boldsymbol{q}_0$ is the initial state and $\mathbb{N}$ is the set of nonnegative integers. For $t \in [t_k, t_{k+1})$, we have $\sigma(t) = \iota_k$, i.e. the ι_k-th subsystem is active. For any $j \in \mathcal{I}$, $\Sigma \mid j = \{t_{j_1}, t_{j_1+1}, \ldots, t_{j_\nu}, t_{j_\nu+1}, \ldots\}$ is the sequence of switching times when the j-th subsystem is "switched on" or "switched off", with $\mathrm{E} \mid j = \{t_{j_1}, \ldots, t_{j_\nu}, \ldots\}$ the "switched on" times of the j-th subsystem.

Theorem 1: ([23]-Theorem 3.9) Assume that for each $j \in \mathcal{I}$, there exists a positive definite generalized Lyapunov-like function $V_j(\boldsymbol{q})$ with respect to $\boldsymbol{f}_j(\boldsymbol{q}, 0)$ and the associated trajectory $\boldsymbol{q}(t)$. Then the origin of the system $\dot{\boldsymbol{q}} = \boldsymbol{f}_\sigma(\boldsymbol{q}, \boldsymbol{u}_\sigma)$, with $\boldsymbol{u}_\sigma \equiv 0$, is stable if and only if there exist class $\mathcal{GK}$ functions α_j satisfying $V_j\left(\boldsymbol{q}(t_{j_{k+1}})\right) - V_j\left(\boldsymbol{q}(t_{j_1})\right) \leq \alpha_j(\|\boldsymbol{q}_0\|)$, $k \geq 1$, $j = 1, \ldots, \chi$.

This theorem states that stability is ensured as long as the change of V_j between any "switched on" time $t_{j_{k+1}}$ and the first active time t_{j_1} is bounded by a class $\mathcal{GK}$ function, regardless of the initial value $V_j\left(\boldsymbol{q}(t_{j_1})\right)$.

Lemma 3: The position $\boldsymbol{r}$ of the switched system $\dot{\boldsymbol{q}} = \boldsymbol{f}_\sigma(\boldsymbol{q}, \boldsymbol{\psi}_\sigma)$, where $\sigma \in \mathcal{I} = \{1, 2, 3\}$, under the proposed switching logic, is Lyapunov stable.

Proof: The correctness of the proposed lemma can be verified by a direct application of Theorem 1. Note that the initial condition $\boldsymbol{r}(0)$ may either be in K or in G, and that all the switchings occur when the state $\boldsymbol{q}$ crosses the switching surface $\mathcal{S} : \|\boldsymbol{r}\| = r_0$. For each subsystem $\sigma \in \{1, 2, 3\}$, consider the generalized Lyapunov-like function $V_\sigma(\boldsymbol{r}) = \|\boldsymbol{r}\|$. Note that V_σ serves as a generalized Lyapunov-like function even when $\sigma = 2$ or $\sigma = 3$ is the active subsystem, i.e. when $\boldsymbol{r}(t) \in G$, since its value is bounded in the sense that $V_\sigma(\boldsymbol{r}(t)) \leq \phi\left(V_\sigma(\boldsymbol{r}(t_k))\right) = \phi(r_0)$, where $t \in [t_k, t_{k+1})$ and $\phi(\cdot) = \|\boldsymbol{r}\|$. At any "switched on" time instant $t_{\sigma n}$ with $n > 1$, (that is, for any "switched on" time instant after the first switch has occurred at $t_{\sigma 1}$), one has that $V_\sigma(\boldsymbol{r}(t_{\sigma n})) \leq r_\sigma$, where $r_\sigma = r_0 + \epsilon_\sigma$ and $\epsilon_\sigma > 0$ can be chosen arbitrarily small. Then, for any first active time $t_{\sigma 1}$, where clearly $V_\sigma(\boldsymbol{r}(t_{\sigma 1})) \geq 0$, one has $V_\sigma(\boldsymbol{r}(t_{\sigma n})) - V_\sigma(\boldsymbol{r}(t_{\sigma 1})) \leq r_\sigma$, that is, any growth of each V_σ is always bounded. ∎

In summary, the trajectories $\boldsymbol{r}(t)$ of the perturbed system (1) are ε-practically asymptotically stable around the origin, with $\varepsilon = r_1$, in the sense that $\boldsymbol{r}(t)$ converge into a ball $\mathcal{B}(\mathbf{0}, r_1)$, where $r_1 = r_0 + \epsilon$ and $\epsilon > 0$ arbitrarily small, and remain into the ball for $t > T$, whereas the orientation θ is regulated to zero when the subsystem $\boldsymbol{f}_3(\boldsymbol{q}, \boldsymbol{\psi}_3)$ is active.

D. Robustness consideration

The control design and stability analysis has been based on the assumption that the disturbance $\boldsymbol{v}$ is known. This is quite unrealistic for the application considered in this paper, since on-line measurements of the current velocity can not be easily acquired. An estimation of the current velocity $\hat{\boldsymbol{v}} = \begin{bmatrix} \hat{v}_x & \hat{v}_y \end{bmatrix}^{\mathrm{T}}$ can be obtained using nonlinear observers and then employed into the control design; however, this complicates the system analysis, since both the estimation error $\tilde{\boldsymbol{v}} = \hat{\boldsymbol{v}} - \boldsymbol{v}$ and $\boldsymbol{q}$ are required to be stable at zero.

Therefore, guaranteeing the robustness of the switched system in the case that the current disturbance is unknown is meaningful for the application considered here. Robustness reduces into guaranteeing that the system trajectories still enter and remain into a ball $\mathcal{B}(\mathbf{0}, \varepsilon)$ of the origin. Assume that only a maximum velocity bound $\|\boldsymbol{v}\|_{\max}$ on the disturbance is known, i.e. that the magnitude of the current velocity $\|\boldsymbol{v}\| = \sqrt{{v_x}^2 + {v_y}^2} \leq \|\boldsymbol{v}\|_{\max}$, while the current direction $\theta_c = \operatorname{atan2}(v_y, v_x)$ is unknown and *not necessarily constant*. In this case, the vector $\boldsymbol{p_p}$ which generates the vector field can not be a priori determined; let us therefore consider the nominal vector field $\mathbf{F_n} = \mathbf{F}$, generated by $\boldsymbol{p_n} = \boldsymbol{p} = \begin{bmatrix} p & 0 \end{bmatrix}^{\mathrm{T}}$, where $p > 0$. Then, applying the proposed switching control strategy is not straightforward, since the terms $\operatorname{sgn}(\boldsymbol{r}^{\mathrm{T}} \boldsymbol{v})$ and $\operatorname{sgn}(v_x)$ are unknown.

Regarding the control law $\boldsymbol{u} = \boldsymbol{\psi}_1(\boldsymbol{q})$, one can verify that, following the same analysis as in the Appendix A, still gets the four cases in terms of $\operatorname{sgn}(\boldsymbol{r}^{\mathrm{T}} \boldsymbol{v})$ and $\operatorname{sgn}(\boldsymbol{p}^{\mathrm{T}} \boldsymbol{r})$, which end up in the conditions (7) and (8). These conditions can be combined to yield

$$\left| \|\boldsymbol{v}\| - \frac{\|\mathbf{F}\|}{\gamma_1(\|\boldsymbol{r}\|)} \right| < k_1 \|\boldsymbol{r}\|, \tag{6}$$

which essentially means that whatever the term $\operatorname{sgn}(\boldsymbol{r}^{\mathrm{T}} \boldsymbol{v})$ is, the system trajectories enter $\mathcal{B}(\mathbf{0}, r_0)$, i.e. the position $\boldsymbol{r}$ robustly converges into $\mathcal{B}(\mathbf{0}, r_0)$ under any current disturbance $\boldsymbol{v}$ such that $\|\boldsymbol{v}\| \leq \|\boldsymbol{v}_{\max}\|$, as long as r_0 satisfies (6).

However, controlling the switched system while being in $\mathcal{B}(\mathbf{0}, r_0)$ depends on both the $\operatorname{sgn}(\boldsymbol{r}^{\mathrm{T}} \boldsymbol{v})$ and the $\operatorname{sgn}(v_x)$, which is included in $\boldsymbol{u} = \boldsymbol{\psi}_2(\boldsymbol{q})$. Nevertheless, the same idea for the control design in $\mathcal{B}(\mathbf{0}, r_0)$ can be used, where now the linear velocity controller depends on the sign of the coordinate x_{in} where the vehicle enters $\mathcal{B}(\mathbf{0}, r_0)$: while in $\mathcal{B}(\mathbf{0}, r_0)$, the vehicle is controlled with $u_1 = -\operatorname{sgn}(x_{\text{in}}) k_3 \|\boldsymbol{v}\|_{\max} > 0$ and $u_2 = -k_4 \theta$, $k_4 > 0$, until it reaches the boundary of $\mathcal{B}(\mathbf{0}, r_0)$. In both cases, a high gain $k_3 > 1$ on the linear velocity u_1 is needed to counteract the destabilizing effect of the unknown lateral velocity induced by the current. At any case, even if the vehicle exits $\mathcal{B}(\mathbf{0}, r_0)$, the control law $\boldsymbol{u} = \boldsymbol{\psi}_1$ guarantees that it will re-enter.

V. Simulation Results

The efficacy of the switching control strategy has been demonstrated through computer simulations. Consider the red triangle in Fig. 4(b), 5(b) as a unicycle-like underwater or surface vehicle (e.g. an underactuated Remotely Operated Vehicle or a hovercraft), that is moving on the horizontal plane under the influence of an environmental disturbance $\boldsymbol{v}$. The goal configuration $\boldsymbol{q_G}$ is the origin and the black line centered at $(0.5, 0)$ is a point of interest, e.g. a target that the vehicle has to inspect through an onboard camera.

Two cases are considered; in the first one the disturbance is known: $\boldsymbol{v} = \begin{bmatrix} -0.1 & 0.2 \end{bmatrix}^{\mathrm{T}}$ m/sec; thus $\boldsymbol{p} = \begin{bmatrix} 0.1 & -0.2 \end{bmatrix}^{\mathrm{T}}$. In the second one, the same disturbance $\boldsymbol{v}$ is assumed to

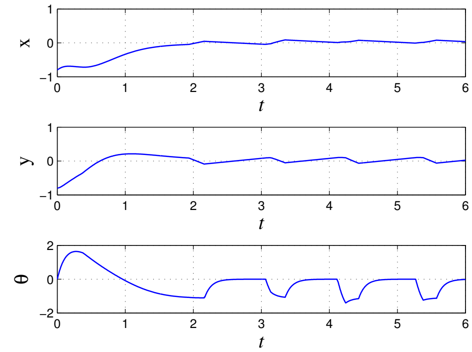

(a) The system trajectories $x(t), y(t), \theta(t)$

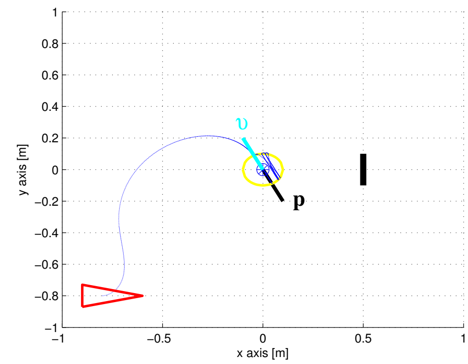

(b) The path $x(t), y(t)$ followed by the system

Fig. 4. System response for *known* $\boldsymbol{v} = \begin{bmatrix} -0.1 & 0.2 \end{bmatrix}^{\mathrm{T}}$

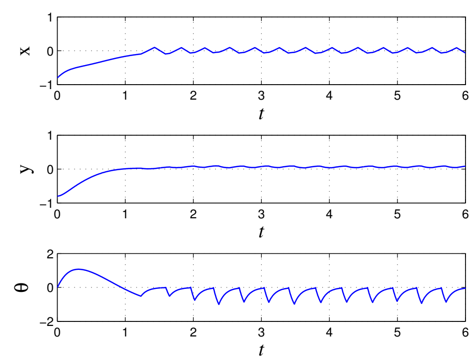

(a) The system trajectories $x(t), y(t), \theta(t)$

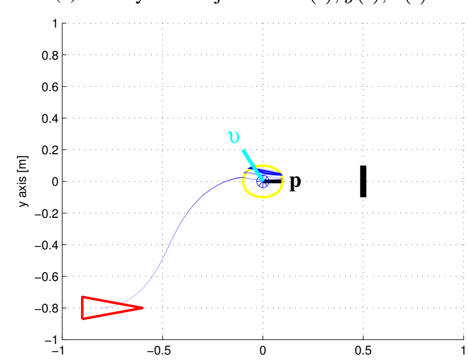

(b) The path $x(t), y(t)$ followed by the system

Fig. 5. System response for *unknown* $\boldsymbol{v} = \begin{bmatrix} -0.1 & 0.2 \end{bmatrix}^{\mathrm{T}}$

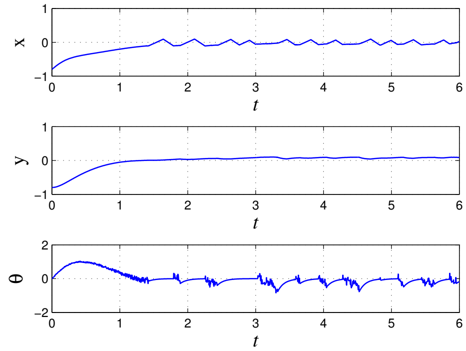

(a) The system trajectories $x(t), y(t), \theta(t)$

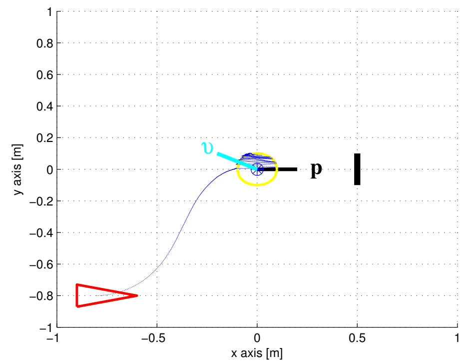

(b) The path $x(t), y(t)$ followed by the system

Fig. 6. System response for *unknown* $\boldsymbol{v}$ under measurement noise

be unknown; the only information available to the switching controller is the velocity bound $\|\boldsymbol{v}\|_{\max}$. The region G is defined as the ball $\mathcal{B}(\mathbf{0}, r_0)$, where $r_0 = 0.1$ m satisfies the conditions (7) and (8). In both cases, the trajectories $x(t)$, $y(t)$ converge into $\mathcal{B}(\mathbf{0}, r_0)$ and remain bounded into the ball $\mathcal{B}(\mathbf{0}, r_1)$, where $r_1 = r_0 + \epsilon$, see Fig. 4(a), 4(b), 5(a), 5(b).

The main difference between the two cases is the evolution of the orientation $\theta(t)$ in the set G; when the disturbance is known, θ is regulated between zero (when $\boldsymbol{u} = \boldsymbol{\psi}_3$ is active) and the direction $\theta_{\boldsymbol{p}}$ of the vector $\boldsymbol{p}$ (when $\boldsymbol{u} = \boldsymbol{\psi}_2$ is active), where $\theta_{\boldsymbol{p}} = \theta_e$. The smaller the component $|v_y|$ is compared to $|v_x|$, the less oscillation occurs for θ. On the contrary, when the current disturbance is unknown, the orientation θ is still regulated to zero, but oscillates with higher frequency: the system switches more frequently between controllers 1 and 3, since the destabilizing effect of the current-induced motion along the unactuated d.o.f. drives the vehicle faster out of the set G, compared to the first case. The hysteresis logic prevents the appearance of chattering when crossing the switching surface.

State-dependent switching is sensitive to measurement noise. In Fig. 6 the state variables are subject to zero-mean, uniform random noise. The system converges into $\mathcal{B}(\mathbf{0}, r_0)$, however chattering occurs during some time intervals around the switching surface. Using some additional control logic, for instance to sample and hold each value of the controls for a long enough period of time, in order to move sufficiently away from the switching surface, may also offer robustness w.r.t. measurement errors.

VI. Conclusions

This paper presented a switching control approach for the practical stabilization of a unicycle-like marine vehicle under non-vanishing, current-induced perturbations. The proposed control scheme is a hysteresis-based switching among three control laws. The first control law employs a dipole-like vector field and drives the system trajectories into a set G around the origin. The other two control laws are active in G; switching between them renders the position of the vehicle practically stable, while the orientation is regulated to zero during some time intervals. The system is robust in the sense that it converges and remains into G, even when only a bound on the perturbation is given. Future work will be on the consideration of input constraints (i.e. thrust saturation) and state constraints (induced by always keeping the target on the camera field-of-view), towards the formulation of the practical stabilization problem for a class of underactuated systems into a viability framework.

Appendix

A. *Controller 1*

Proof: (Lemma 1) Define the dipole moment $\boldsymbol{p}_{\mathbf{p}} = \boldsymbol{p} = \begin{bmatrix} p_1 & p_2 \end{bmatrix}^{\mathrm{T}}$ such that $\boldsymbol{p}^{\mathrm{T}} \hat{\boldsymbol{x}}_{\mathcal{G}} > 0 \Rightarrow p_1 > 0$, so that the direction of the flow lines at $(0,0)$ is $\theta_{\mathbf{p}} \in [-\pi/2, \pi/2]$. Thus, take $\boldsymbol{p} = \begin{bmatrix} v_x \operatorname{sgn}(v_x) & v_y \operatorname{sgn}(v_x) \end{bmatrix}^{\mathrm{T}}$, which implies that if $v_x \geq 0$, then $\boldsymbol{p} = \boldsymbol{v}$, whereas if $v_x < 0$, then $\boldsymbol{p} = -\boldsymbol{v}$.

Define the orientation error $\eta = \theta - \varphi$, where φ is the orientation of the field (2) at (x, y), and consider the error dynamics $\dot{\eta} = \dot{\theta} - \dot{\varphi} \Rightarrow \dot{\eta} = u_2 - \dot{\varphi}$. Substituting the control law (3b) yields $\dot{\eta} = -k_2(\theta - \varphi) + \dot{\varphi} - \dot{\varphi} \Rightarrow \dot{\eta} = -k_2 \eta$, which implies that θ converges exponentially to φ.

To study the convergence of the trajectories $\boldsymbol{r}(t)$ into a ball $\mathcal{B}(\mathbf{0}, r_0)$, consider the Lyapunov function $V = \frac{1}{2}(x^2 + y^2)$, which is positive definite, radially unbounded and of class C^1 and take the derivative of V along the trajectories of (1),

$$\dot{V} = \nabla V \begin{bmatrix} \dot{x} \\ \dot{y} \end{bmatrix} = \begin{bmatrix} x & y \end{bmatrix} \begin{bmatrix} u_1 \cos\theta + v_x \\ u_1 \sin\theta + v_y \end{bmatrix} = \boldsymbol{r}^{\mathrm{T}} \begin{bmatrix} \cos\theta \\ \sin\theta \end{bmatrix} u_1 + \boldsymbol{r}^{\mathrm{T}} \begin{bmatrix} v_x \\ v_y \end{bmatrix}.$$

Substituting the control law (3a) eventually yields

$$\dot{V} = -k_1 \left| \boldsymbol{r}^{\mathrm{T}} \begin{bmatrix} \cos\theta \\ \sin\theta \end{bmatrix} \right| \|\boldsymbol{r}\| + \operatorname{sgn}(\boldsymbol{r}^{\mathrm{T}} \boldsymbol{v}) |\boldsymbol{r}^{\mathrm{T}} \boldsymbol{v}| - \left(\boldsymbol{r}^{\mathrm{T}} \begin{bmatrix} \cos\theta \\ \sin\theta \end{bmatrix} \right) \operatorname{sgn}(\boldsymbol{r}^{\mathrm{T}} \boldsymbol{v}) \operatorname{sgn}(\boldsymbol{p}^{\mathrm{T}} \boldsymbol{r}) \|\boldsymbol{v}\|.$$

C1. If $\operatorname{sgn}(\boldsymbol{p}^{\mathrm{T}} \boldsymbol{r}) = -1$ and $\operatorname{sgn}(\boldsymbol{r}^{\mathrm{T}} \boldsymbol{v}) = 1$, then

$$\dot{V} = -k_1 \left| \boldsymbol{r}^{\mathrm{T}} \begin{bmatrix} \cos\theta \\ \sin\theta \end{bmatrix} \right| \|\boldsymbol{r}\| + |\boldsymbol{r}^{\mathrm{T}} \boldsymbol{v}| + \left(\boldsymbol{r}^{\mathrm{T}} \begin{bmatrix} \cos\theta \\ \sin\theta \end{bmatrix} \right) \|\boldsymbol{v}\|.$$

Moreover, since under (3b) one has $\dot{\eta} = -k_2 \eta$, one can argue that by choosing $k_2 > 0$ large enough, the orientation error $\eta \to 0 \Rightarrow \theta \to \varphi$ fast enough, compared to the rest (slow) dynamics. In this case, $\boldsymbol{r}^{\mathrm{T}} \begin{bmatrix} \cos\varphi \\ \sin\varphi \end{bmatrix} \leq 0$. Thus,

$$\dot{V} = -\left| \boldsymbol{r}^{\mathrm{T}} \begin{bmatrix} \cos\varphi \\ \sin\varphi \end{bmatrix} \right| (k_1 \|\boldsymbol{r}\| + \|\boldsymbol{v}\|) + \left| \boldsymbol{r}^{\mathrm{T}} \boldsymbol{v} \right|.$$

After some algebra one can verify that

$$\left| \boldsymbol{r}^{\mathrm{T}} \begin{bmatrix} \cos\varphi \\ \sin\varphi \end{bmatrix} \right| = \|\mathbf{F}\|^{-1} \left| \boldsymbol{r}^{\mathrm{T}} \begin{bmatrix} \mathrm{F}_{px} \\ \mathrm{F}_{py} \end{bmatrix} \right| = \|\mathbf{F}\|^{-1} \left| \boldsymbol{r}^{\mathrm{T}} \boldsymbol{v} \right| \gamma_1(\|\boldsymbol{r}\|),$$

where $\gamma_1(\|\boldsymbol{r}\|) = \lambda \|\boldsymbol{r}\|^2 - 1 + e^{-\|\boldsymbol{r}\|^2}$ is of class $\mathcal{K}_\infty$ for $\lambda \geq 2$, the norm $\|\mathbf{F}\|$ of the field is zero only at $\boldsymbol{r} = \mathbf{0}$ and

$$\|\mathbf{F}\| = \sqrt{\lambda (\boldsymbol{r}^{\mathrm{T}} \boldsymbol{v})^2 \left(\lambda \|\boldsymbol{r}\|^2 - 2(1 - e^{-\|\boldsymbol{r}\|^2}) \right) + \|\boldsymbol{v}\|^2 \left(1 - e^{-\|\boldsymbol{r}\|^2} \right)^2}.$$

Then, $\dot{V} = \left|\boldsymbol{r}^{\mathrm{T}}\boldsymbol{v}\right|\left(1 - \|\mathbf{F}\|^{-1}\gamma_1(\|\boldsymbol{r}\|)\left(k_1\|\boldsymbol{r}\| + \|\boldsymbol{v}\|\right)\right)$, where the second factor is negative for

$$\|\mathbf{F}\|^{-1}\gamma_1(\|\boldsymbol{r}\|)\left(k_1\|\boldsymbol{r}\| + \|\boldsymbol{v}\|\right) > 1. \tag{7}$$

C2. If $\operatorname{sgn}(\boldsymbol{p}^{\mathrm{T}}\boldsymbol{r}) = -1$ and $\operatorname{sgn}(\boldsymbol{r}^{\mathrm{T}}\boldsymbol{v}) = -1$, then

$$\dot{V} = -k_1\left|\boldsymbol{r}^{\mathrm{T}}\left[\begin{smallmatrix}\cos\theta\\ \sin\theta\end{smallmatrix}\right]\right|\|\boldsymbol{r}\| - \left|\boldsymbol{r}^{\mathrm{T}}\boldsymbol{v}\right| - \left(\boldsymbol{r}^{\mathrm{T}}\left[\begin{smallmatrix}\cos\theta\\ \sin\theta\end{smallmatrix}\right]\right)\|\boldsymbol{v}\|.$$

Considering $\theta = \varphi$, in this case $\boldsymbol{r}^{\mathrm{T}}\left[\begin{smallmatrix}\cos\varphi\\ \sin\varphi\end{smallmatrix}\right] \le 0$. Then,

$\dot{V} = -\left|\boldsymbol{r}^{\mathrm{T}}\left[\begin{smallmatrix}\cos\varphi\\ \sin\varphi\end{smallmatrix}\right]\right|\left(k_1\|\boldsymbol{r}\| - \|\boldsymbol{v}\|\right) - \left|\boldsymbol{r}^{\mathrm{T}}\boldsymbol{v}\right|$, which yields $\dot{V} = -\left|\boldsymbol{r}^{\mathrm{T}}\boldsymbol{v}\right|\left(1 + \|\mathbf{F}\|^{-1}\gamma_1(\|\boldsymbol{r}\|)\left(k_1\|\boldsymbol{r}\| - \|\boldsymbol{v}\|\right)\right)$,

where the second factor is positive for

$$\|\mathbf{F}\|^{-1}\gamma_1(\|\boldsymbol{r}\|)\left(k_1\|\boldsymbol{r}\| - \|\boldsymbol{v}\|\right) > -1. \tag{8}$$

C3. If $\operatorname{sgn}(\boldsymbol{p}^{\mathrm{T}}\boldsymbol{r}) = 1$ and $\operatorname{sgn}(\boldsymbol{r}^{\mathrm{T}}\boldsymbol{v}) = 1$, then $\dot{V}$ is the same as in C1, thus it is ≤ 0 if (7) holds.
C4. If $\operatorname{sgn}(\boldsymbol{p}^{\mathrm{T}}\boldsymbol{r}) = 1$ and $\operatorname{sgn}(\boldsymbol{r}^{\mathrm{T}}\boldsymbol{v}) = -1$ then $\dot{V}$ is the same as in C2, thus it is ≤ 0 if (8) holds.

In summary, one has $\dot{V} \le 0$ for any $\boldsymbol{r}$ that satisfies (7), (8), and $\dot{V} = 0$ if and only if $\boldsymbol{r}^{\mathrm{T}}\boldsymbol{v} = 0$. Thus, for $\boldsymbol{r}^{\mathrm{T}}\boldsymbol{v} \ne 0$, any initial $\boldsymbol{r}(0)$ and any $0 < r_0 < \|\boldsymbol{r}(0)\|$ that satisfy (7) and (8), $\dot{V}$ is negative in the set $\{\boldsymbol{r} \mid \frac{1}{2}{r_0}^2 \le V(\|\boldsymbol{r}\|) \le \frac{1}{2}\|\boldsymbol{r}(0)\|^2\}$, which verifies that $\boldsymbol{r}(t)$ enters the set $\{\boldsymbol{r} \mid V(\boldsymbol{r}) \le \frac{1}{2}{r_0}^2\}$, i.e. $\boldsymbol{r}(t)$ enters the ball $\mathcal{B}(\mathbf{0}, r_0)$ under the control law (3b), as long as θ converges exponentially to φ under the control law (3b). Note that the case $\boldsymbol{r}^{\mathrm{T}}\boldsymbol{v} = 0$ does not affect the convergence of the system into $\mathcal{B}(\mathbf{0}, r_0)$. ■

B. Controller 2

Proof: (Lemma 2) Under the control law (4) the system trajectory hits the boundary $\partial G_{1_{G_2}}$ and then the boundary ∂G_{2_B}. To verify the first argument, consider

$$V_{21} = \boldsymbol{r}^{\mathrm{T}}\boldsymbol{v} + \frac{1}{2}(\theta - \theta_{\mathbf{p}})^2 = x v_x + y v_y + \frac{1}{2}(\theta - \theta_{\mathbf{p}})^2,$$

which is positive for $\boldsymbol{r} \in G_1$ and zero on $\partial G_{1_{G_2}}$ with $\theta = \theta_{\mathbf{p}}$, and take its time derivative along the system trajectories,

$$\dot{V}_{21} = -\boldsymbol{v}^{\mathrm{T}}\left[\begin{smallmatrix}\cos\theta\\ \sin\theta\end{smallmatrix}\right] k_3 \operatorname{sgn}(v_x)\|\boldsymbol{v}\| + \|\boldsymbol{v}\|^2 - k_4(\theta - \theta_{\mathbf{p}})^2.$$

Consider $\operatorname{sgn}(v_x) = -1$ and assume that the system has reached G_1 with $\boldsymbol{v}^{\mathrm{T}}\left[\begin{smallmatrix}\cos\theta\\ \sin\theta\end{smallmatrix}\right] < 0$. Then, $\dot{V}_{21} = \|\boldsymbol{v}\|\left(\|\boldsymbol{v}\| - k_3\left|\boldsymbol{v}^{\mathrm{T}}\left[\begin{smallmatrix}\cos\theta\\ \sin\theta\end{smallmatrix}\right]\right|\right) - k_4(\theta - \theta_{\mathbf{p}})^2$, where the first term is < 0 for $k_3 > 1$, whereas $\dot{V}_{21} = 0 \Leftrightarrow \{k_3 = 1$ and $\theta = \theta_{\mathbf{p}}\}$. Then, for $k_3 > 1$ the system trajectory starting in G_1 enters the region G_2. Similarly one can verify the case $\operatorname{sgn}(v_x) = 1$, for $\boldsymbol{v}^{\mathrm{T}}\left[\begin{smallmatrix}\cos\theta\\ \sin\theta\end{smallmatrix}\right] > 0$. For the second argument, consider $V_{22} = {r_0}^2 - \|\boldsymbol{r}\|^2 = {r_0}^2 - (x^2 + y^2)$, which is positive for $\boldsymbol{r} \in G_2$ and zero on ∂G_{2_B}. The time derivative of V_{22} along the system trajectories is $\dot{V}_{22} = -2\boldsymbol{r}^{\mathrm{T}}\left[\begin{smallmatrix}\cos\theta\\ \sin\theta\end{smallmatrix}\right] u_1 - 2\boldsymbol{r}^{\mathrm{T}}\boldsymbol{v}$. For $\operatorname{sgn}(v_x) = -1$: $\boldsymbol{r}^{\mathrm{T}}\boldsymbol{v} < 0$ and $\boldsymbol{r}^{\mathrm{T}}\left[\begin{smallmatrix}\cos\theta\\ \sin\theta\end{smallmatrix}\right] > 0$. Then, $\dot{V}_{22} = 2\|\boldsymbol{v}\|\left(\|\boldsymbol{r}\| - k_3\left|\boldsymbol{r}^{\mathrm{T}}\left[\begin{smallmatrix}\cos\theta\\ \sin\theta\end{smallmatrix}\right]\right|\right)$, which is < 0 for $\|\boldsymbol{r}\| < k_3\left|\boldsymbol{r}^{\mathrm{T}}\left[\begin{smallmatrix}\cos\theta\\ \sin\theta\end{smallmatrix}\right]\right| \le \|\boldsymbol{r}\| \Rightarrow k_3 > 1$. Thus, for $k_3 > 1$, the system hits the boundary ∂G_{2_B} and enters B. For $\operatorname{sgn}(v_x) = 1$: $\boldsymbol{r}^{\mathrm{T}}\boldsymbol{v} < 0$ and $\boldsymbol{r}^{\mathrm{T}}\left[\begin{smallmatrix}\cos\theta\\ \sin\theta\end{smallmatrix}\right] < 0$. Following the same procedure, $\dot{V}_{22} < 0 \Rightarrow k_3 > 1$. ■

References

[1] C. Canudas de Wit and H. Khennouf, "Quasi-continuous stabilizing controllers for nonholonomic systems: Design and robustness considerations," in *Proc. of the 3rd European Control Conference*, Rome, Italy, Sep. 1995, pp. 2630–2635.

[2] Z.-P. Jiang, "Robust exponential regulation of nonholonomic systems with uncertainties," *Automatica*, vol. 36, pp. 189–209, 2000.

[3] W. E. Dixon, D. M. Dawson, E. Zergeroglu, and A. Behal, "Robustness to kinematic disturbances," in *Nonlinear Control of Wheeled Mobile Robots*, ser. Lecture Notes in Control and Information Sciences. Springer Berlin / Heidelberg, 2001, vol. 262, pp. 113–130.

[4] D. A. Lizarraga, N. P. I. Aneke, and H. Nijmeijer, "Robust point stabilization of underactuated mechanical systems via the extended chained form," *SIAM Journal on Control and Optimization*, vol. 42, no. 6, pp. 2172–2199, 2003.

[5] S. Ge, Z. Wang, and T. Lee, "Adaptive stabilization of uncertain nonholonomic systems by state and output feedback," *Automatica*, vol. 39, pp. 1451–1460, 2003.

[6] C. Prieur and A. Astolfi, "Robust stabilization of chained systems via hybrid control," *IEEE Transactions on Automatic Control*, vol. 48, no. 10, pp. 1768–1772, Oct. 2003.

[7] Y. Guo, "Nonlinear H_∞ control of uncertain nonholonomic systems in chained forms," *International Journal of Intelligent Control and Systems*, vol. 10, no. 4, pp. 304–309, Dec. 2005.

[8] Y. Wu and X. Zheng, "Robust stabilization of uncertain nonholonomic systems with strong nonlinear drifts," *Journal of Control Theory and Applications*, vol. 6, no. 4, pp. 427–430, Nov. 2008.

[9] M. L. Corradini, T. Leo, and G. Orlando, "Robust stabilization of a mobile robot violating the nonholonomic constraint via quasi-sliding modes," in *Proc. of the American Control Conference*, San Diego, California, Jun. 1999, pp. 3935–3939.

[10] S. S. Ge, J. Wang, T. H. Lee, and G. Y. Zhou, "Adaptive robust stabilization of dynamic nonholonomic chained systems," *Journal of Robotic Systems*, vol. 18, no. 3, pp. 119–133, 2001.

[11] P. Lucibello and G. Oriolo, "Robust stabilization via iterative state steering with an application to chained-form systems," *Automatica*, vol. 37, pp. 71–79, 2001.

[12] P. Morin and C. Samson, "Practical stabilization of driftless systems on Lie groups: The transverse function approach," *IEEE Transactions on Automatic Control*, vol. 48, no. 9, pp. 1496–1508, Sep. 2003.

[13] T. Floquet, J.-P. Barbot, and W. Perruquetti, "Higher-order sliding mode stabilization for a class of nonholonomic perturbed systems," *Automatica*, vol. 39, pp. 1077–1083, 2003.

[14] E. Valtolina and A. Astolfi, "Local robust regulation of chained systems," *Systems and Control Letters*, vol. 49, pp. 231–238, 2003.

[15] X. Zhu, G. Dong, Z. Cai, and D. Hu, "Robust simultaneous tracking and stabilization of wheeled mobile robots not satisfying nonholonomic constraint," *Journal of Central South University of Technology*, vol. 14, no. 4, pp. 537–545, Aug. 2007.

[16] K. Y. Pettersen and T. I. Fossen, "Underactuated dynamic positioning of a ship - experimental results," *IEEE Trans. on Control Systems Technology*, vol. 8, no. 5, pp. 856–863, Sep. 2000.

[17] K. Y. Pettersen and H. Nijmeijer, "Semi-global practical stabilization and disturbance adaptation for an underactuated ship," *Modeling, Identification and Control*, vol. 22, no. 2, pp. 89–101, Apr. 2001.

[18] A. P. Aguiar and A. M. Pascoal, "Dynamic positioning and way-point tracking of underactuated AUVs in the presence of ocean currents," *Int. Journal of Control*, vol. 80, no. 7, pp. 1092–1108, Jul. 2007.

[19] A. Pereira, J. Das, and G. S. Sukhatme, "An experimental study of station keeping on an underactuated ASV," in *Proc. of the 2008 IEEE/RSJ Int. Conf. on Intelligent Robots and Systems*, Nice, France, Sep. 2008, pp. 3164–3171.

[20] D. Panagou, H. G. Tanner, and K. J. Kyriakopoulos, "Dipole-like fields for stabilization of systems with Pfaffian constraints," in *Proc. of the 2010 IEEE International Conference on Robotics and Automation*, Anchorage, Alaska, May 2010, pp. 4499–4504.

[21] A. P. Aguiar, J. P. Hespanha, and A. M. Pascoal, "Switched seesaw control for the stabilization of underactuated vehicles," *Automatica*, vol. 43, pp. 1997–2008, 2007.

[22] M. S. Branicky, "Multiple Lyapunov functions and other analysis tools for switched and hybrid systems," *IEEE Transactions on Automatic Control*, vol. 43, no. 4, pp. 475–482, Apr. 1998.

[23] J. Zhao and D. J. Hill, "On stability, L_2-gain and H_∞ control for switched systems," *Automatica*, vol. 44, pp. 1220–1232, 2008.